Book of Tutorials and Abstracts

European Microbeam Analysis Society

EMAS 2019

16th

EUROPEAN WORKSHOP

on

MODERN DEVELOPMENTS AND APPLICATIONS IN MICROBEAM ANALYSIS

19 to 23 May 2019
at the
NTNU, Realfagbygget
Trondheim, Norway

Organised in collaboration with:
Norwegian University of Science and Technology
(NTNU)

DEVELOPMENT AND VALIDATION OF STANDARDLESS AND STANDARDS-BASED X-RAY MICROANALYSIS

Philippe T. Pinard, A. Protheroe, J. Holland, S. Burgess and P.J. Statham

Oxford Instruments NanoAnalysis Ltd.
Halifax Road, HP12 3SE High Wycombe, Great Britain
e-mail: philippe.pinard@oxinst.com

Dr. Philippe Pinard graduated with a PhD in Engineering from the RWTH Aachen in Germany. He joined Oxford Instruments in 2016 as a Microanalysis Technologist within the Research group. Philippe focusses his research on EDS, WDS and EBSD, in particular the development and improvement of these analytical techniques. He is author or co-author of 32 papers in international journals and 16 conference presentations including 3 invited talks.

1. INTRODUCTION

In its simplest expression, quantification in electron probe microanalysis (EPMA) is the conversion of X-ray intensities to a composition. The relationship between the measured intensity ($I_{j,k}$) of an X-ray line (k) of an element (j) and its mass fraction (c_j) is given by the fundamental X-ray intensity:

$$I_{j,k} = c_j \frac{N_A}{M_j} \frac{i\tau}{e} \frac{\Omega}{4\pi} \varepsilon_{j,k} p_{j,k} f_{j,k}(\vec{c}, E_0, \psi) \quad (1)$$

where N_A is Avogadro's number, M, the molar mass, i, the beam current, τ, the acquisition time, e, the elementary charge, Ω, the solid angle, ε, the efficiency of the detector, p, the radiative transition probability combining the fluorescence yield, Coster-Kronig transition and line weight, $f_{j,k}(\vec{c}, E_0, \psi)$, the X-ray emission calculated for a given X-ray line (j,k), composition ($\vec{c}$), accelerating voltage (E_0) and take-off angle of the detector (ψ). The X-ray emission model, also known as a matrix correction, defines the emission probability of an X-ray line under the analytical conditions used to measure the X-ray intensity. For simplicity, the subscripts j and k will be omitted in the following equations.

Castaing's k-ratio [1], Cliff-Lorimer's k-factor [2] or any other quantification approaches in X-ray microanalysis have been designed to simplify Eq. 1 by cancelling out some terms and developing theoretical models to calculate others. Looking at the k-ratio, the normalisation of the intensity (I_{unk}) from an unknown sample by the one of a standard material (I_{std}) eliminates all terms that are not dependent on the concentration:

$$k = \frac{I_{unk}}{I_{std}} = \frac{c_{unk}}{c_{std}} \frac{\cancel{N_A/M}}{\cancel{N_A/M}} \frac{\cancel{i\tau/e}}{\cancel{i\tau/e}} \frac{\cancel{\Omega/4\pi}}{\cancel{\Omega/4\pi}} \frac{\cancel{\varepsilon p}}{\cancel{\varepsilon p}} \frac{f(\vec{c}_{unk}, E_0, \psi)}{f(\vec{c}_{std}, E_0, \psi)} = \frac{c_{unk} f'(\vec{c}_{unk}, E_0, \psi)}{c_{std} f'(\vec{c}_{std}, E_0, \psi)} \quad (2)$$

assuming that the electron dose ($i\tau$) is either the same or measured during the acquisition of both X-ray intensities. Note that the normalisation also simplifies the X-ray emission model ($f \rightarrow f'$) since only the relative emission probability must be calculated (i.e., without the ionisation cross-section). Starting from Castaing, authors have developed different theoretical models in other to calculate the remaining term, $f(\vec{c}, E_0, \psi)$, including ZAF correction, $\varphi(\rho z)$ models and Monte Carlo simulation programmes . The quantification therefore combines an empirical and theoretical method, the normalisation by a standard intensity and the calculation of the X-ray emission probability. This combination is a key strength of EPMA in comparison to other analytical techniques as it provides an accurate quantification of a wide range of samples with a general and reproducible experimental method.

EPMA is not however without limitations and caveats. The measurement of X-ray intensities on standard samples entails the procurement of these standards (covering all the elements to be analysed) as well as the expertise to evaluate, store and maintain them. The quantification can only be as accurate as the accuracy of the standards. This means that the standards must be

properly characterised to assess their composition, homogeneity, flatness, electrical conductivity, etc. This assessment should also be verified over time to check for any degradation (segregation, oxidation, etc.). These complications and requirements related to standards along with the desire to improve the usability and efficiency of quantitative analyses led to the development of standardless quantification approaches [3-6].

While it is often described as an inaccurate, unverifiable "black box" [7-9], standardless quantification is equally derived from Eq. 1, but uses different methods to cancel out unknown terms and calculate others in order to convert measured X-ray intensities to a composition. As selected methods can vary, this may explain the discrepancies between the different approaches. In the following paragraphs, we would like to describe the methods used in one approach to standardless quantification for energy-dispersive X-ray spectrometry (EDS) including how X-ray intensities are extracted from ED spectra. We will then present experimental work to validate the accuracy of the standardless quantification with the latest generation silicon drift detector (SDD).

2. *METHOD*

2.1. *Standardless quantification*

As stated above standardless quantification aims to eliminate the need of every characterisation laboratory to buy and maintain a series of standards and, therefore, lower the barrier to quantitative X-ray microanalysis. One obvious solution is to calculate X-ray intensities directly from Eq. 1 without the need of any standard. While it is an important research topic to further improve the understanding of electron-photon-matter interactions, the first-principle approach is very susceptible to inaccuracies in the physical parameters and models. A more practical approach is to still rely on the acquisitions of standard X-ray intensities (Eq. 2), but to transfer the expertise and responsibility of the standard acquisition to someone else. In other words, the standard X-ray intensities are acquired on another system than the one used to acquire the X-ray intensities from an unknown sample.

Let us define the following scenario where the unknown X-ray intensities are acquired on a system labelled "user" and the standard X-ray intensities on a system labelled "factory". Because the acquisitions on one system likely use different analytical conditions (detector, accelerating voltage, beam current, etc.) than on the other, fewer terms cancel out in the *k*-ratio equation (Eq. 2):

$$k = \frac{I_{unk}}{\mathbf{I_{std}}} = \frac{c_{unk}}{\mathbf{c_{std}}} \frac{\cancel{N_A/M}}{\cancel{N_A/M}} \frac{i\tau/e}{\mathbf{i\tau/e}} \frac{\Omega/\cancel{4\pi}}{\mathbf{\Omega/4\pi}} \frac{\varepsilon}{\boldsymbol{\varepsilon}} \frac{p}{\boldsymbol{p}} \frac{f(\vec{c}_{unk},E_0,\psi)}{f(\vec{\mathbf{c}}_{std},\mathbf{E_0},\boldsymbol{\psi})} = \frac{c_{unk} i\tau\Omega\varepsilon f(\vec{c}_{unk},E_0,\psi)}{c_{std} \mathbf{i\tau\Omega\varepsilon} f(\vec{\mathbf{c}}_{std},\mathbf{E_0},\boldsymbol{\psi})} \quad (3)$$

where the bold, grey terms indicate those corresponding to the factory system. The acquisition

time and accelerating voltage are known quantities as they are selected by the user. The port geometry of the X-ray detector on the electron microscope specifies its take-off angle. The value is normally fixed and known from the engineering drawing. The beam current, solid angle, detector efficiency, X-ray emission model and standard intensity are the remaining unknown terms in Eq. 3, obviously besides the concentration of the measured element in the unknown sample.

Use of a Faraday cup, either inserted inside the electron column or mounted on the stage, is the classical method to measure the beam current. In contrast to electron probes, scanning electron microscopes (SEM) rarely have the equipment required to measure a beam current (ammeter, stage connection, etc.). It is much harder to experimentally determine the solid angle. Even with the correct formulation [10] and all the information regarding the sensor (area, shape, entry angle), the sensor to sample distance is often unknown and may change depending on the acquisition conditions (e.g., X-ray detector may be retracted to avoid collision with other detectors inside the microscope).

Several approaches to standardless quantification require the normalisation of the quantification results. The additional equation, $\sum c_i = 1$, effectively eliminates the need to measure $i\Omega/\Omega$ since it is a constant in the *k*-ratio equation of all measured elements for a given acquisition. Normalisation is a double-edged sword. On one hand it allows an easy assessment of the composition of a sample, on the other hand, it hides potentially serious experimental errors (charging, omission of elements, etc.).

One approach to avoid normalisation and obtain unnormalised quantification results is to calibrate both the user and factory system using an acquisition on a pure sample. This calibration resembles the *k*-ratio approach, except that the X-ray intensities in the numerator and denominator are not from the same X-ray line. The X-ray intensities only need to be acquired by the same X-ray detector under the same analytical conditions (i.e., accelerating voltage, beam current, insertion distance). For example, Cu-K and Zn-K X-ray intensities from an unknown brass sample can be calibrated using the Co-K X-ray intensity from a pure Co sample. The calibration acts exactly as a beam current measurement, meaning that it can be repeated to check the beam current stability or if the beam current was changed. The calibration also removes out the solid angle term from Eq. 3:

$$\frac{I_{unk}}{I_{cal}} = \frac{c_{unk}}{\cancel{c_{cal}}} \frac{\cancel{N_A/M}}{\cancel{N_A/M}} \frac{\cancel{i\tau/e}}{\cancel{i\tau/e}} \frac{\cancel{\Omega/4\pi}}{\cancel{\Omega/4\pi}} \frac{\varepsilon_{unk}}{\varepsilon_{cal}} \frac{p_{unk}}{p_{cal}} \frac{f(\vec{c}_{unk},E_0,\psi)}{f(\vec{c}_{cal},E_0,\psi)} \tag{4}$$

The calibration is performed on a pure standard, so c_{cal} is unity. In contrast to the *k*-ratio (Eq. 2), the radiative transition probabilities (p and p_cal) do not cancel out because two different X-ray lines are used. If the same calibration is performed on the factory system using the same element, the radiative transition probabilities are removed, and Equation 3 becomes:

$$k = \frac{I_{unk} I_{cal}}{I_{std} I_{cal}} = \frac{c_{unk} \varepsilon_{unk} \varepsilon_{cal} \cancel{p_{unk} p_{cal}} f(\vec{c}_{unk}, E_0, \psi) f(\vec{c}_{cal}, E_0, \psi)}{c_{std} \varepsilon_{std} \varepsilon_{cal} \cancel{p_{std} p_{cal}} f(\vec{c}_{std}, E_0, \psi) f(\vec{c}_{cal}, E_0, \psi)} \quad (5)$$

It is, however, not a requirement that the same calibration sample is used on the user and factory system. In that case, the X-ray intensities of the two calibration samples measured on the factory system are used to construct an additional ratio based on rearranging the terms of Eq. 4. For this ratio, all terms are known and multiplying it to Eq. 5 results in the cancellation of the radiative transition probability terms since they are independent of the system. Equation 5, therefore, demonstrates that it is possible to indirectly measure the beam current without a Faraday cup and cancel out the solid angle regardless of the geometry of the X-ray detector and its position inside the microscope.

It is likely that the detector efficiency will be different between the user and factory system if X-ray detectors from different generations are used. For a given system, the efficiency between the X-ray line of the unknown and calibration element could also be very different. In the results presented below, the detector efficiency is derived from a direct measurement of the efficiency of a "gold standard" Si(Li)-detector using the Bessy II synchrotron in Berlin [11]. Before and after the synchrotron measurements, X-ray intensities from standard samples were acquired using the same detector on a SEM where the take-off angle of the detector was carefully measured by tilting a sample surface away from the detector. Microscope conditions (beam current, accelerating voltage) were carefully monitored during these acquisitions. For any new type of X-ray detector (e.g., new SDD), a new model for the efficiency curve is constructed based on the synchrotron and SEM measurements of the gold standard detector, as well as an intimate knowledge of the manufacturing processes, window characteristics and detector parameters. The model is adjusted using X-ray intensities measured using the new X-ray detector, where its efficiency (ε) at the energy of the measured X-ray line is given by:

$$\varepsilon = \frac{I}{I_{cal}} \frac{I_{cal}^{GS}}{I^{GS}} \varepsilon_{GS} \quad (6)$$

where the subscript *GS* indicates X-ray intensities measured by the "gold standard" detector. As shown in Statham 2009 [12] and 2010 [13], the experimental efficiency determined by the synchrotron significantly improves the standardless quantification results, especially for the quantification using X-ray lines below 1 keV (e.g., O-K and F-K).

As in the standard-based *k*-ratio equation (Eq. 2), a model must be used to calculate the X-ray emission model and correct for matrix effects in the X-ray emission between the unknown and standard samples. In the standardless *k*-ratio equation (Eq. 5) this model is also used to correct for differences in the calibration measurement between the user and factory systems. In all the following results, the X-ray emission is calculated using the $\varphi(\rho z)$ model, XPP, as described in Pouchou and Pichoir (1991) [14].

Finally, the remaining undetermined quantity is the X-ray standard. Using the factory system, X-ray intensities from a series of standards, consisting of pure elements and simple binaries (e.g., SiO_2, FeS_2), were acquired at two accelerating voltages: 5 and 20 kV. The take-off angle of the X-ray detector, thickness of carbon coating on standard block, homogeneity of standards, etc., were carefully measured prior to the measurements. As described above, a calibration standard was periodically measured, Co for the acquisitions at 20 kV and Si for those at 5 kV, instead of a direct measurement of the beam current. The X-ray intensities from the standards were then stored as ratios to the Co-K or Si-K X-ray intensity to produce a "factory" standards database.

This completes the description of the standardless quantification approach. Comparing Eqs. 2 and 5 illustrates the similitudes between standard-based quantification and this approach. Both calculate a *k*-ratio of each analysed element, both correct for matrix effects using a $\varphi(\rho z)$ model, both use the same iterative procedure to solve for the unknown concentrations and both output unnormalised quantification results. Both approaches can also be combined if needed. The trade-off between the two approaches could be summarised as the requirement for well-characterised standards versus a well-characterised X-ray detector.

2.2. Extraction of X-ray intensity

Besides the quantification method, one important consideration is how to accurately extract X-ray intensities from an ED spectrum in order to calculate the *k*-ratios (Eq. 2 or 5). This applies to both standard-based or standardless quantification. Extracting X-ray intensities is a multi-step process which typically involves:

1. Correction of the energy scale;
2. Correction of artefacts peaks;
3. Removal of the background;
4. Fit of modelled or experimental peak profiles over the X-ray peaks of interest;
5. Extract X-ray intensity from the fitted X-ray peak.

In some pulse processing electronics, a "strobe zero" peak is obtained by accumulating a histogram of measurements that would be obtained from zero-energy photons. The measurement is performed in time gaps between real X-ray events using exactly the same pulse processing as for a real event. By fitting a Gaussian to this histogram, the channel position for zero energy photons is determined without needing a special standard. This position can be used first to calibrate the energy scale using a single X ray peak from an element standard and is subsequently used on every spectrum to correct for any shift in zero position. With the proper gain calibration of the electronics, this ensures that all X-ray peaks appear at the right energy in the ED spectrum.

Silicon escape and pulse pile-up peaks are artefacts from the X-ray detection [9]. While different phenomena cause these artefact peaks, both results in the reduction of the X-ray intensity of the parent peak. They may also indirectly affect other X-ray peaks as they can coincide with other

"real" X-ray peaks and artificially increase their X-ray intensity. Besides the X-ray intensity, these artefact peaks may lead to the misidentification of elements in the spectrum, which would inevitably influence the accuracy of the quantification results. For these three reasons, it is important to correct these artefacts before extracting the X-ray intensities of any peak. This especially applies to acquisitions at high count rates where the influence of pulse pile-up peaks increases. Silicon escape peaks can be corrected using algorithms developed by Reed and Ware [15] and improved by Statham [16] to consider the enhanced resolution of the escape peak, whereas Statham [17, 18]) and Eggert *et al.* [19, 20]) describe the principles of pulse pile-up correction.

The X-ray intensity terms in all the previous equations more precisely refer to the intensity from the emission of characteristic X-ray lines. This implies stripping the background from the ED spectrum, i.e., removing the contribution of Bremsstrahlung X-rays from the spectrum. From the literature, two methods have been proposed for this operation: (1) fitting a calculated background to the experimental and (2) filtering out the background using a convolution filter (also known as top-hat filter) [21-24]. The first method requires the composition of the analysed area to calculate the background as well as peak-free background points to adjust the calculated background. While the composition can iteratively be determined, any misidentification of the X-ray peaks (e.g., Si instead of Ta) would result in an incorrect background shape due to the different absorption behaviour. The second method, the convolution filter, was thus selected as it offers a consistent and operator-independent way to remove the background for any spectrum, including spectra with no clear peak-free background region, for example the 100 - 1,000 eV region in Fig. 1. The convolution filter is automatically adjusted to match the X-ray detector resolution to ensure the accurate filtering of the background for all samples at any X-ray energy. Nonetheless, the calculated background can be a useful tool to validate the element identification and the quantification results [25].

The resolution of EDS entails that X-ray lines from different elements may overlap. The X-ray peaks must be separated before extracting their respective X-ray intensities. This is normally performed using least-squares fitting of the experimental spectrum (after background removal) with either experimental [23] or calculated peak profiles [22, 24] (Fig. 2). If a convolution filter is used to remove the background, this means that the least-squares fitting is performed between the filtered experimental spectrum and the filtered peak profiles. In practise, calculated peak profiles offer more flexibility as they implicitly take into account the influence of the acquisition conditions (e.g., accelerating voltage, X-ray detector resolution and pulse processor settings). The model must however properly describe the impulse response function of the X-ray detector (i.e., charge collection, efficiency, etc.) and construct peak profiles based on accurate fundamental data of relative line weights, mass absorption coefficients and Coster-Kronig transitions [16, 25]. This is particularly true for L and M X-ray line series with large absorption edges within the line series.

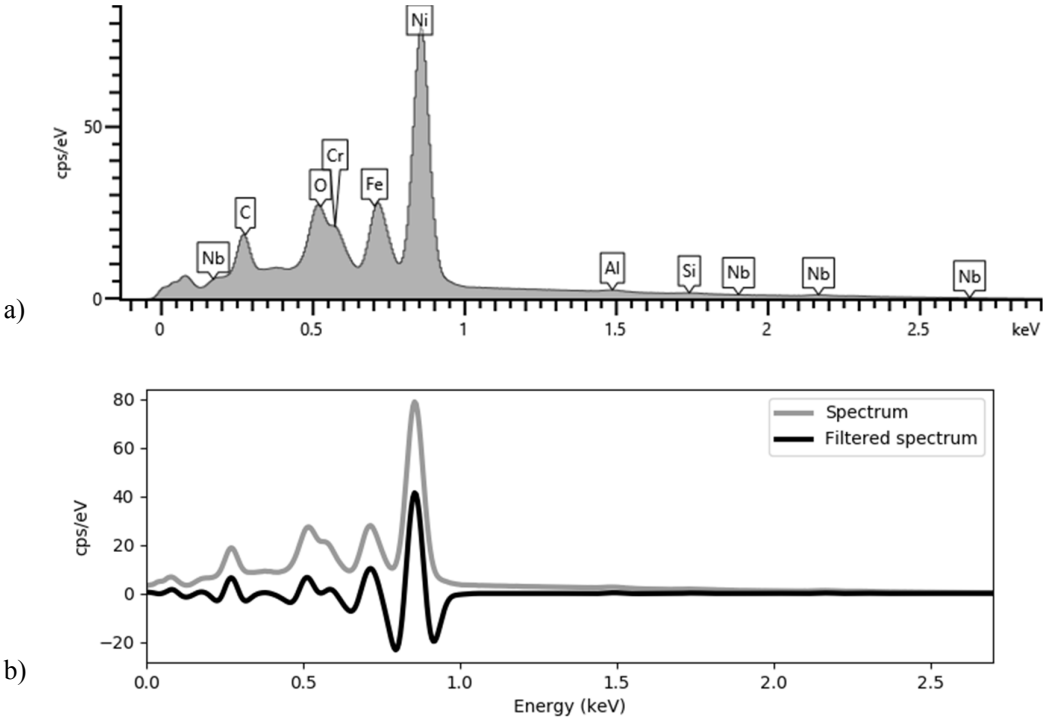

Figure 1. a) Spectrum of a 718-steel alloy acquired at 3 kV (Zeiss Merlin, X-Max Extreme detector, 1.3 nA, PT4, 600 s live time), and b) after applying the convolution filter. Sample is courtesy of Manchester University.

The least-squares fitting is always performed over the whole X-ray line series. In other words, all X-ray lines emitted by the transition to a specific shell (i.e., K, L, M, etc.) are fitted together. This is because X-ray lines from the same family often overlap at the EDS resolution. While several parameters could be included in the least-square fitting (e.g., resolution, relative line weights, peak positions), this would quickly result in ambiguous solutions. A more robust strategy is to only fit the relative area ratio of the overlapping X-ray line series. For a given X-ray line series, its experimental area is thus the product of the line series profile area and the fitted relative ratio.

In Eqs. 2 and 5, the detector efficiency and X-ray emission model are normally defined either at a specific X-ray energy and for a specific X-ray line. In other words, the value of these quantities may differ between the X-ray lines within a same family. In contrast to wavelength-dispersive X-ray spectrometry (WDS), the line series area (or peak height) cannot directly be used as the X-ray intensity in the k-ratio equation [23]. One method to convert line series areas ($I_{j,\sum k}$) to an X-ray intensity ($I_{j,k}$) is to determine the most intense X-ray line in the family (k') and calculate its contribution to the line series area:

$$I_{j,k'} = I_{j,\sum k} \frac{\hat{I}_{j,k'}}{\hat{I}_{j,\sum k}} \tag{7}$$

a)

b)

c)

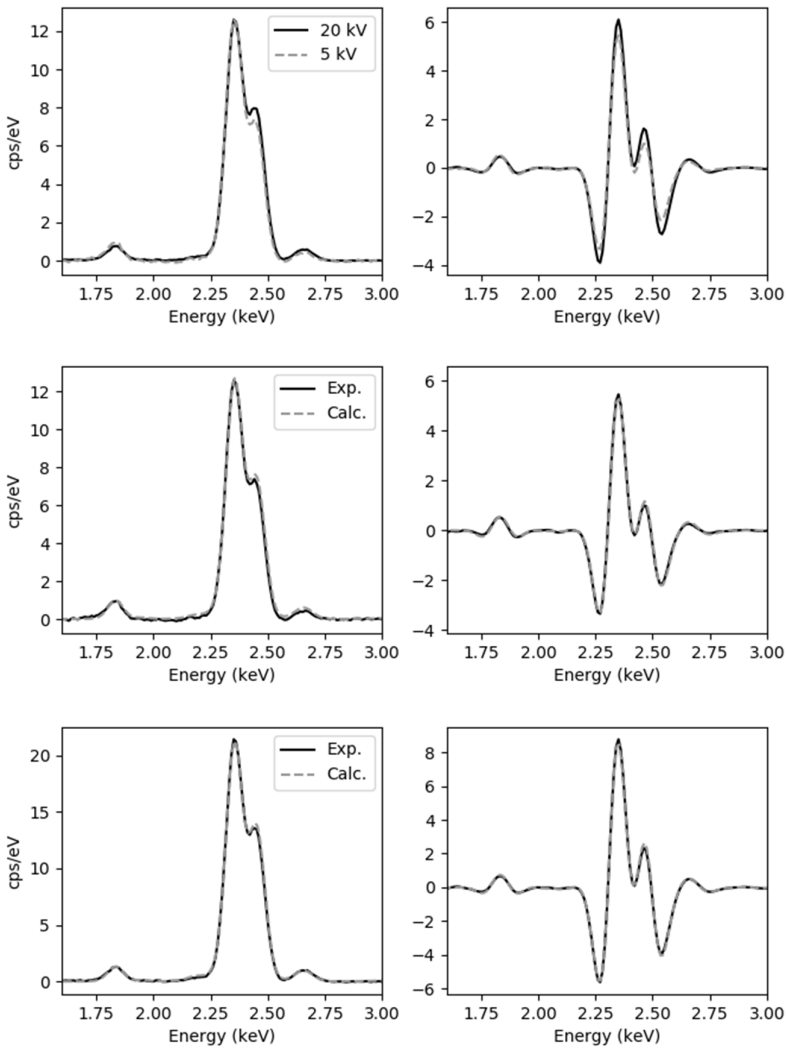

Figure 2. a) Comparison between experimental spectra of Pb-M X-ray line series acquired at 5 and 20 kV (X-MaxN 80, PT5, 100 s live time ,10 eV/ch). Comparison of these experimental spectra with calculated peak profile at b) 5 kV, and c) 20 kV. The background was removed from the left spectra, whereas the right spectra correspond to the raw experimental spectra after the convolution filter.

where $\hat{I}_{j,k'}$ and $\hat{I}_{j,\sum k}$ are respectively the calculated intensity for the most intense X-ray line (k') of element j and the calculated area of its corresponding family.

This concludes the description of how X-ray intensities are extracted from ED spectra, regardless whether standard-based or standardless quantification is used. It is worth pointing out that regardless of strategies used to extract X-ray intensities, theoretical models for X-ray emission and detection are required (e.g., background model, peak profile model, pulse pile-up correction). It is not possible to purely rely on empirical methods to extract X-ray intensities

from ED spectra. This contrasts with WDS where X-ray intensities correspond to the peak height subtracted by a background intensity interpolated from two off-peak measurements.

3. EXPERIMENTAL PROCEDURE

To assess the accuracy of the standardless quantification approach, experimental ED spectra were acquired on 53 standard samples, part of a single standard block (#6260, Micro-Analysis, Consultants Ltd., St Ives, United Kingdom). The standard samples include pure elements, simple binaries (SiO_2, HgTe, InAs, Fe_3C, GaP, FeS_2, NaCl, etc.) and minerals (albite, orthoclase, wollastonite). In contrast to standard-based quantification, the standardless quantification of pure element standards is a good indicator of the accuracy of the detector efficiency and the matrix correction if the factory standards were acquired using a different X-ray detector and/or under different analytical conditions. The standard block was carbon-coated by the manufacturer. Using the thin-film measurement tool, LayerProbe (Oxford Instruments, High Wycombe, United Kingdom), the carbon thickness was measured on some of the standards and found to be uniform and equal to 13.5 nm on average. The oxide thickness was less than 5 nm on most of the metallic standards, except on Ti and V where the oxide thickness was 13 and 30 nm, respectively. At the accelerating voltage used, this level of oxidation should have minimal influence on the quantification results.

ED spectra were acquired using a single Oxford Instruments Ultim Max 100 SDD with a Mn resolution of 127 eV at an input count rate of 130 kcps. The detector was installed on a Leo 1450VP scanning electron microscope (Zeiss, Oberkochen, Germany). The elevation is 35° at a working distance of 20 mm. The channel width was fixed at 10 eV/channel (2,048 channels and 20 keV energy range). Three sets of acquisitions were performed at different accelerating voltages (15 and 20 kV) and input count rates (50 and 200 kcps). Table 1 summarises the acquisition conditions. Since the X-ray emission is sample dependent, the input count rate (ICR) was adjusted on pure Co where the dead time was kept at 30 % by changing the process time. The live time was similarly adjusted to approximately acquire 1 million counts on Co irrespectively of the input count rate (ICR).

Table 1. Analytical conditions for accuracy tests.

	Test A	**Test B**	**Test C**
Accelerating voltage (kV)	20	15	20
Input count rate (kcps) on Co	50	50	200
Approx. beam current on Co (nA)	1.25	1.25	4.98
Live time (s)	20	20	5
Process time	PT5	PT5	PT3
Dead time on Co (%)	~30	~30	~30

Cobalt was used as the calibration element. The measurement on Co was repeated after every 5 - 7 acquisitions on the standard samples to minimise the effect of any beam current instability. The same acquisition conditions were used, except that the total number of counts in the spectra was set to 600,000.

The spectrum processing to extract X-ray intensities and the quantification were performed using AZtec v4.1. All spectra were escape peak and pulse pile-up corrected. Elements in each spectrum were automatically identified. Any trace elements (< 1 wt%) [26] were excluded from the analysis as the counting time was not sufficient to properly measure these elements. Unless otherwise stated, all elements were quantified by direct measurement, including oxygen of the measured oxides and minerals. The X-ray line used for quantification was automatically selected by the software based on the overvoltage. All results use standardless quantification method and are unnormalised.

The experimental procedure described above follows the one previously performed by Burgess *et al.* [27] and Statham [12] with an input count rate of 10 kcps.

4. RESULTS AND DISCUSSION

In the following figures, the standardless "unnormalised" quantification results are compared to the nominal compositions specified by the manufacturer of the standard block. The comparison is performed by taking the ratio between the measured and nominal concentration. A value close to unity indicates a good agreement, whereas a value below or above respectively implies an underestimation or overestimation of the concentration by the standardless quantification. The results are plotted as a histogram centred at unity with a fixed scale between 0.8 and 1.2 (i.e., ± 20 % relative deviation). Any ratio falling outside this range is separately reported and excluded from the overall average and standard deviation.

4.1. Test A (20 kV, 50 kcps)

Figure 3a shows the results for the acquisitions with an accelerating voltage of 20 kV and an input count rate on Co of 50 kcps. There is one outlier, B in LaB_6, with a ratio of 1.2066. All other 75 measured concentrations are within 20 % of the nominal concentrations, including 68 within 5%. This yields a well-centred distribution with a relative error of 3.3 %. The concentrations with a relative deviation greater than 5 % generally correspond to those of light elements (B, O and N).

The overall relative error drops to 2.1 % if the analysis of light elements is excluded. This relative error approaches the rule of thumb value of 2 %, usually quoted when describing the accuracy of EPMA performed by WDS, as well as the one of 1.8 % obtained by Pouchou and Pichoir [14], when developing the XPP $\varphi(\rho z)$ models. While more exhaustive than this work,

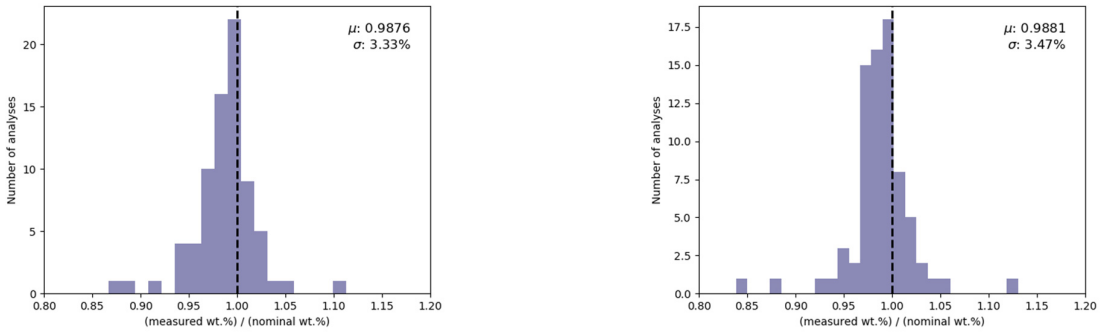

a) b)

Figure 3. Comparison of measured and nominal quantification results acquired with an accelerating voltage of 20 kV, an input count rate on Co of 50 kcps, a live time of 20 s and PT5 process time. The standard block was rotated by 180° in (b)..

their analysis of 826 *k*-ratios also excluded those of light elements. Inaccuracies in the X-ray emission model, or more precisely the mass absorption coefficients, and in the peak profile model might explain the larger errors in the quantification of light elements.

Overall, the results demonstrate that standardless quantification can achieve an accuracy of 5 % or better without any special settings or adjustment to the "user" system. It likewise confirms the accuracy of the strategy used to extract X-ray intensities from the spectra.

The measurements were repeated twice (Figs. 3a and 3b), with the stage rotated by 180° for the second set. Besides confirming the results, this technique provides a way to verify that the standard block is flat and therefore, that the take-off angle is roughly equal to the elevation.

4.2. Test B (15 kV, 50 kcps)

The experiment was repeated at an accelerating voltage of 15 kV. As shown in Fig. 4 the relative standard deviation increases from 3.3 to 4.2 %. B in LaB_6 is no longer an outlier with a ratio of 1.15, which reinforces the aforementioned hypothesis that the larger error might be attributed to inaccuracies in the mass absorption coefficients of light elements (lower absorption correction at 15 kV). Two reasons might explain the increase of the standard deviation between the experiments of Test A and B. Firstly, the overvoltage on the X-ray line used for quantification decreases at 15 kV and thus the measured X-ray intensity. Taking only the analyses with an overvoltage less than 5 at 20 kV (26 concentrations), the relative error increases from 1.9 % at 20 kV to 2.5 % at 15 kV. On average the measured X-ray intensity at 15 kV is approximately 10 % lower than at 20 kV, including more than 30 % drop for X-ray lines of the first-row transition metals. A longer acquisition time for some of these measurements might help improve the results. A second explanation might be due to the inaccuracies in the fundamental parameters used in the X-ray emission model, such as the X-ray ionisation probability or the mass absorption

coefficients. In Test A, some of these inaccuracies cancel out since the unknown and standard samples were measured at the same accelerating voltage. Nonetheless, this experiment again confirms that standardless quantification can determine the composition with an accuracy better than 5 %, even if different analytical conditions are used for the "user" and "factory" system.

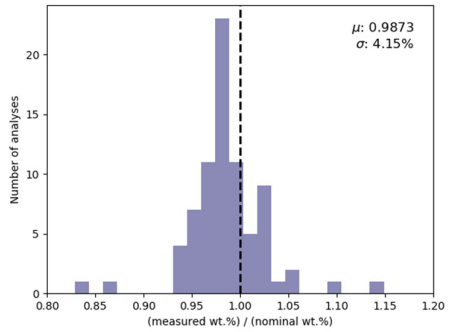

Figure 4. Comparison of measured and nominal quantification results acquired with an accelerating voltage of 15 kV, an input count rate on Co of 50 kcps, a live time of 20 s and PT5 process time.

4.3. Test C (20 kV, 200 kcps)

The results of final test are shown in Fig. 5. Despite a four-fold increase in the input count rate, Test C has a similar relative error than Test A (3.2 versus 3.3 %). There are, however, two additional outliers, N in BN (0.773) and Be in pure Be (1.234). The distribution is also slightly shifted to the left with an average ratio of 0.976 instead of 0.988. This indicates the measured concentrations are on average slightly lower than the nominal concentrations. As the input count rate on some samples can be as high as 330 kcps, an incomplete correction of some pulse pile-up peaks might explain the decrease of the average ratio. The change of process time from Test A did not have an influence on the results, confirming that the associated increase of the resolution to 133 eV was correctly modelled in the calculated peak profile. The similitudes between the results of Test A and C confirm the ability to increase the productivity of quantitative analyses by using standardless quantification at high count rates without sacrificing the accuracy [28].

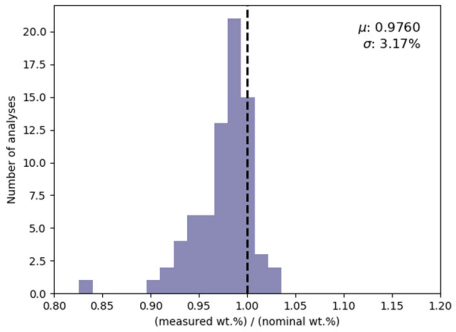

Figure 5. Comparison of measured and nominal quantification results acquired with an accelerating voltage of 20 kV, an input count rate on Co of 200 kcps, a live time of 5 s and PT3 process time.

6. CONCLUSION

Many factors influence the analytical techniques a scientist chooses to characterise his/her samples. One of the factors is certainly the easy of use of the technique, or in more measurable terms, the "time to result". Castaing's PhD-thesis was innovative in many ways, but one crucial realisation is the need of a theoretical model for the X-ray emission. He could have resorted to make different brass standards to quantify his copper-zinc diffusion couple, but he opted to use pure standards and develop the first matrix correction model. The X-ray emission model is key to remove the requirement to find, prepare and measure standards of similar composition to the unknowns. The ability to use pure or simple compounds as standards is a clear advantage of EPMA over other analytical techniques as it generalises and shortens the experimental procedure.

Standardless quantification further simplifies quantitative analyses by removing the need of the user to measure X-ray intensities on standards. The approach used in this work combines a detailed characterisation of X-ray detectors and the production of a factory standards database. Only a measurement on a single standard is required to obtain unnormalised results. The results presented in this and previous works confirm that this approach can achieve an accuracy better than 5 % under different analytical conditions (accelerating voltage, process time and input count rate).

7. REFERENCES

[1] Castaing R 1951 *Application of electron probes to local chemical and crystallographic analysis*. PhD-thesis. (Paris, France: Université de Paris)
[2] Cliff G and Lorimer G W 1975 *J. Microsc.* **103** 203-207
[3] Statham P J 1981 *J. Microsc.* **123** 1-23
[4] Eggert F 1994 *Standardless electron probe microanalysis*. in: EDO conference
[5] Scheller S, Salge T and Terborg R 2010 *Microsc. Microanal.* **16** 1314-1315
[6] Trincavelli J, Limandri S and Bonetto R 2014 *Spectrochim. Acta B* **101** 76-85
[7] Newbury D E 1998 *Microsc. Microanal.* **4** 585-597
[8] Newbury D E 2002 *Microsc. Microanal.* **8** (Suppl. 2) 1464-1465
[9] Goldstein J I, *et al.* 2018 *Scanning electron microscopy and X-ray microanalysis*. (Berlin-Heidelberg, Germany: Springer)
[10] Zaluzec N J 2009 *Microsc. Microanal.* **15** 93-98
[11] Alvisi M, *et al.* 2006 *Microsc. Microanal.* **12** 406-415
[12] Statham P 2009 *Microsc. Microanal.* **15** 528-529
[13] Statham P 2010 *Microsc. Microanal.* **16** 1304-1305
[14] Pouchou J-L and Pouchou F 1991 Quantitative analysis of homogeneous or stratified microvolumes applying the model "PAP". in: *Electron probe quantitation*. (Heinrich K F J and Newbury D E; EDs.) (New York, NY: Plenum Press) 31-75

[15] Reed S J B and Ware N G 1972 *J. Phys. E: Sci. Instrum.* **5** 582-583
[16] Statham P J 2014 *Microsc. Microanal.* **20** 690-691
[17] Statham P J 1977 *X-ray Spectrom.* **6** 94-103
[18] Statham P J 2006 *Microchim. Acta* **155** 289-294
[19] Eggert F, Elam T, Anderhalt R and Nicolosi J 2011 *Microsc. Microanal.* **17** 1192-1193
[20] Eggert F, Elam T, Anderhalt R and Nicolosi J 2012 *IOP Conf. Ser.: Mater. Sci. Engng.* **32** 12008
[21] Statham P J 1977 *Anal. Chem.* **49** 2149-2154
[22] Statham P J 2002 *J. Res. Natl. Inst. Stand. Technol.* **107** 531-546
[23] Ritchie N W M, Newbury D E and Davis J M 2012 *Microsc. Microanal.* **18** 892-904
[24] Terborg R, Salge T, Pinard P T and Richter S 2016 *Microsc. Microanal.* **22** 404-405
[25] Statham P, Penman C and Duncumb P 2016 *IOP Conf. Ser.: Mater. Sci. Engng.* **109** 12016
[26] Newbury D E and Ritchie N W M 2016 *Microsc. Microanal.* **22** 520-535
[27] Burgess S, Statham P, Holland J and Chou Y-H 2007 *Microsc. Microanal.* **13** 1432-1433
[28] Pinard P T, Burgess S, Zhang J Q, Holland J and Statham P 2018 *Microsc. Microanal.* **24** 724-725